Supplemental material to this article can be found at:
http://molpharm.aspetjournals.org/content/suppl/2022/03/31/molpharm.121.000370.DC1
1521-0111/101/6/390–399$35.00
MOLECULAR PHARMACOLOGY
dx.doi.org/10.1124/molpharm.121.000370
Mol Pharmacol 101:390–399, June 2022




# Coassembly of Warm Temperature–Sensitive Transient Receptor Potential Vanilloid (TRPV) 3 and TRPV4 Channel Complexes with Distinct Functional Properties[S]

Fang Hu,[1] Xu Cao,[1] Canyang Niu, and KeWei Wang

*Department of Pharmacology, School of Pharmacy, Qingdao University Medical College, Qingdao, China (F.H., C.N., K.W.); Department of Neurobiology, Neuroscience Research Institute, Peking University Health Science Center, Beijing, China (X.C.); and Institute of Innovative Drugs, Qingdao University, Qingdao, China (K.W.)*

Received July 6, 2021; accepted March 17, 2022

## ABSTRACT

Heteromeric assembly of temperature-sensitive transient receptor potential (TRP) ion channels has been suggested to underlie the molecular basis of fine-tuning of temperature detection and chemical sensation. However, whether warm temperature–sensitive TRP vanilloid (TRPV) 3 and TRPV4 channels robustly expressed in the skin can form heteromeric assembly remains largely unknown. In this study, we show that TRPV3 and TRPV4 channels can coassemble into functional heterotetrameric channels with distinct properties. Confocal imaging reveals a colocalization and association of TRPV3 and TRPV4 proteins in cell membrane. Coimmunoprecipitation analysis demonstrates a strong protein-protein interaction between TRPV3 and TRPV4 subunits from heterogeneously expressed cells or mouse skin tissues through their C termini but not in TRPV3 knockout tissues. Coexpression of TRPV3 and TRPV4 channels yields a heterotetrameric channel complexes characterized by an intermediate single-channel conductance, distinct activation threshold, and pharmacology. Taken together, our findings demonstrate a heterotetrameric assembly of TRPV3 and TRPV4 channels, which may help explain the role of temperature-sensitive TRPV channels in fine-tuning of environmental detection and sensation in the skin.

## SIGNIFICANCE STATEMENT

The coassembly of transient receptor potential vanilloid (TRPV) 3 and TRPV4 channel complexes increases the functional diversity within the channel subfamily, which may serve as a molecular basis for fine-tuning of environmental detection and temperature sensation in mammals.

## Introduction

Thermosensation and chemesthetic sensation, the most ancient sensory processes in mammals, are essential abilities to detect and react to changes in environmental temperature and chemesthesis for survival and function (Bandell et al., 2007; Vriens et al., 2014). The transient receptor potential (TRP) ion channels are activated by a wide range of thermal, chemical, and mechanical stimuli, with several TRP channels with temperature sensitivity known as thermo-TRPs that serve as the principal detectors of thermosensation and chemesthesis (Dhaka et al., 2006; Bandell et al., 2007; Nilius and Owsianik, 2011; Vay et al., 2012; Kashio, 2021). TRP melastatin 8 (TRPM8) and TRP ankyrin 1 (TRPA1) are activated by nonpainful cool temperatures and painful cold, respectively (Peier et al., 2002a; Laursen et al., 2015). TRP vanilloid (TRPV) 1 and 2 channels detect painful levels of heat (Caterina et al., 1997, 1999), and TRPM2–5, TRPV3, and TRPV4 are activated by nonpainful warmth (Güler et al., 2002; Peier et al., 2002b; Smith et al., 2002; Xu et al., 2002; Talavera et al., 2005; Vriens et al., 2011; Tan and McNaughton, 2016). Then, the questions arise as to whether and how the thermo-TRPs can associate to form heterotetrameric channels that are able to fine-tune thermosensation and temperature detection. Elucidating the details of molecular basis of thermosensation will provide crucial insight into the physiology and pharmacology of thermosensitivity and thermoregulation.

Heteromeric assembly of subunits is a widespread mechanism underlying the diversity of the TRP channel family. Heteromeric channels exhibit unique biophysical functions and pharmacological properties for sensation and adaption of various environmental stimuli. Heteromeric assembly of TRP channel subunits was first demonstrated between TRP and

This work was supported by the National Natural Science Foundation of China [Grant 31701019] (to F.H.) and [Grant 81973299] (to K.W.) and by the Ministry of Science and Technology of China [Grant 2018ZX09711001-004-006].

No author has an actual or perceived conflict of interest with the contents of this article.

[1]F.H. and X.C. contributed equally to this work.

dx.doi.org/10.1124/molpharm.121.000370.

[S] This article has supplemental material available at molpharm.aspetjournals.org.

**ABBREVIATIONS:** 2-APB, 2-aminoethoxydiphenyl borate; ARD, ankyrin repeat domain; CT, C terminus; EYFP, enhanced yellow fluorescent protein; Gap43, growth-associated protein 43; HEK, human embryonic kidney; KO, knockout; $n_{Hill}$, Hill slope; pS, picosiemens; TRAAK, TWIK-related arachidonic acid–stimulated $K^+$; TREK, TWIK-related $K^+$; TRP, transient receptor potential; TRPC, TRP canonical; TRPL, TRP-like protein; TRPM, TRP melastatin; TRPP, TRP polycystic; TRPV, TRP vanilloid; TRPV3-H426N/R696K, two double mutations of H426N and R696K in TRPV3 background; TRPV4-N456H/W737R, two double mutations of N456H and W737R in TRPV4 background; WT, wild-type.

TRP-like protein (TRPL) in *Drosophila melanogaster*, which leads to cation currents with unique permeation properties and low constitutive activity (Xu et al., 1997). Additionally, various complexes of heteromeric TRP channels can be formed, including heteromers of TRP canonical (TRPC)1 and TRPC3 (Lintschinger et al., 2000), TRP$\gamma$ and TRPL (Xu et al., 2000), TRPC1 and TRPC5 (Strübing et al., 2001), TRPM6 and TRPM7 (Li et al., 2006), and TRP polycystic (TRPP)2 and TRPC1 (Bai et al., 2008). Among the thermo-TRPV subunits, heteromeric TRPV1/3 channels exhibit single-channel conductance and chemical activation and temperature sensitivity that are distinct from their homomeric channels (Cheng et al., 2007, 2012). However, whether TRPV3 and TRPV4 channels can coassemble remains largely unaddressed.

Both TRPV3 and TRPV4 channels are predominantly expressed in sensory neurons and keratinocytes of the skin (Güler et al., 2002; Peier et al., 2002b; Smith et al., 2002; Xu et al., 2002). In mice, TRPV3 is expressed in the keratinocytes of the skin (Peier et al., 2002b), and TRPV3 mRNAs and proteins are also found in the sensory neurons in primates (Smith et al., 2002; Xu et al., 2002; Szöllősi et al., 2018). TRPV4 is highly expressed in the rodent skin and sensory nerve fibers, especially in the suprabasal keratinocytes (Güler et al., 2002; Lapajne et al., 2020). Both TRPV3 and TRPV4 share a high overall sequence similarity of about 42% (Güler et al., 2002; Smith et al., 2002). Despite their coexistence in the same cell and structural similarity, TRPV3 and TRPV4 feature distinct functional properties. TRPV3 is activated by warm temperature at a threshold of 32–39°C with robust currents at elevated temperatures (Peier et al., 2002b; Smith et al., 2002; Xu et al., 2002). TRPV4 is activated by warm temperature with a threshold of 25°C and a shallower temperature-response profile (Güler et al., 2002; Watanabe et al., 2002). TRPV3 is sensitized to repeated stimuli, whereas TRPV4 is desensitized (Peier et al., 2002b; Watanabe et al., 2002). It is of interest that gain-of-function mutations in TRPV3 cause Olmsted Syndrome, characterized by palmoplantar and periorificial keratoderma and severe itching (Lin et al., 2012). Similarly, patients with a heterozygous mutation in TRPV4 also show scaly skin (Liu et al., 2020), a phenotype similar to newborn TRPV3$^{-/-}$ mice with dry, reddened, and scaly skin (Cheng et al., 2010). All of these observations suggest that TRPV3 and TRPV4 channels may coassemble into heterotetramers involved in the skin physiology and pathology.

In this study, we tested whether TRPV3 and TRPV4 channels can coassemble into functional channel complexes. We show that TRPV3 and TRPV4 can form channel complexes via the association of their C termini. Coexpression of TRPV3 and TRPV4 subunits results in heterotetrameric assembly with an intermediate single-channel conductance, altered pharmacology, and distinct temperature activation threshold.

## Materials and Methods

**Plasmids and Constructs.** For confocal fluorescence microscopy, mouse TRPV3 (BC108984.1) and mouse TRPV4 (NM_022017.3) cDNAs were inserted into an enhanced yellow fluorescent protein (EYFP)-N3 vector with EYFP fused at the channel C terminus (TRPV3-EYFP) or pLVX-mCherry-N1 vector with mCherry fused at the channel N terminus (mCherry-TRPV4). Mouse TRPV3 C terminus (TRPV3 CT, residues 709–791) and ankyrin repeat domain (TRPV3 ARD, residues 118–367) were cloned into vector EYFP-N3 with EYFP fused at the C terminus (TRPV3 CT-EYFP, TRPV3 ARD-EYFP). Mouse TRPV4 C terminus (TRPV4 CT, residues 749–871) and ARD domain (TRPV4 ARD, residues 149–396) were cloned into pcDNA3.1(+) vector with growth-associated protein 43 (Gap43) fused at the N terminus (Gap43-TRPV4 CT, Gap43-TRPV4 ARD). For immunoprecipitation analysis, mouse TRPV3 and mouse TRPV4 cDNAs were inserted into an EYFP-N3 vector (TRPV3-EYFP) or pcDNA3.1(+) vector with three tandem-repeated Flag epitopes (DYKDDDDK) at the channel N terminus (Flag-TRPV4). For electrophysiological recordings, mouse TRPV3 and mouse TRPV4 cDNAs or their mutants were inserted into a pcDNA3.1(+) vector. For pharmacology tests, two double mutations were generated: TRPV4-N456H/W737R (containing N456H and W737R double mutations in TRPV4 background) and TRPV3-H426N/R696K (containing H426N and R696K double mutations in TRPV3 background).

**Confocal Imaging.** Human embryonic kidney (HEK)293 cells were maintained for culture at 37°C under 5% $CO_2$ in Dulbecco's modified Eagle's medium (DMEM) supplemented with 10% fetal bovine serum. For colocalization experiments, HEK293 cells were transfected with TRPV3-EYFP and mCherry-TRPV4 and cotransfected with TRPV3-EYFP/mCherry-TRPV4 constructs using Lipofectamine2000 (11668019; Invitrogen). For analysis of interaction between the channel N-terminal ARD and/or C terminus (CT), HEK293 cells were transfected with TRPV3 CT-EYFP and TRPV3 ARD-EYFP and cotransfected with TRPV3 CT-EYFP/Gap43-TRPV4 CT, TRPV3 CT-EYFP/Gap43-TRPV4 ARD, TRPV3 ARD-EYFP/Gap43-TRPV4 CT, and TRPV3 ARD-EYFP/Gap43-TRPV4 ARD constructs using Lipofectamine2000 (11668019). Twenty-four hours after transfection, HEK293 cells were washed with phosphate-buffered saline (PBS, pH 7.4) three times. The fluorescence signals were observed using Focusing Nosepiece System (Ni-E; Nikon, Tokyo, Japan).

**Immunoprecipitation.** For immunoprecipitation, HEK293 cells transfected with cDNAs of both TRPV3 and TRPV4 in different ratios (1:1, 2:1, 1:2) or individual TRPV3 or TRPV4 were homogenized in ice-cold Radio-Immunoprecipitation Assay (RIPA) buffer (R0020; Solarbio Life Sciences, Beijing, China) containing 50 mM Tris (pH 7.4), 250 mM NaCl, 10 mM EDTA, 0.5% NP-40, and 1 mM phenylmethylsulfonylfluoride (PMSF) using a tissue grinder (SCIENTZ-48; Ningbo Scientz Biotechnology, Zhejiang, China) before being lysed at 4°C for 30 minutes. Cell lysates were centrifuged at 12,000 *g* for 5 minutes at 4°C. Supernatants containing 400 to 500 $\mu$g of proteins were incubated overnight at 4°C with a rabbit anti-TRPV3 antibody (1:100, raised by immunizing rabbits with a protein encoding amino acids 326–340 of mouse TRPV3) or normal rabbit immunoglobulin G (1:200, sc-2028; Santa Cruz Biotechnology) with protein A-Sepharose CL-4B resin (GE Healthcare) in a volume of 500 $\mu$l. The samples were then washed six times with Tris-buffered saline/0.1% Triton X-100 to solubilize bound proteins. The proteins of TRPV3 precipitates were resolved by 10% SDS-PAGE, and TRPV4 proteins were detected in Western blot assay using a mouse anti-Flag antibody (1:2000, F1804; Sigma-Aldrich).

For ex vivo immunoprecipitation, TRPV3$^{-/-}$ mice purchased from The Jackson Laboratory were used. For viability and fertility, TRPV3$^{-/-}$ mice were generated with the construct deleting exons encoding the putative pore region and adjacent transmembrane segments five and six, essential domains of the ion channel, resulting in low levels of truncated TRPV3 transcript (Moqrich et al., 2005). All animal experimental procedures were approved by the Animal Care and Use Committee of Qingdao University, and efforts were made to minimize the discomfort of the animals. Adult male and female mice (8–10 weeks old) were used and deeply anesthetized with 10% chloral hydrate (0.3 g/kg, i.p.). Mouse skin tissues were removed and immediately homogenized in ice-cold RIPA buffer (R0020) using a tissue grinder (SCIENTZ-48) before being lysed at 4°C for 1 hour. Cell lysates were then centrifuged at 12,000 *g* for 5 minutes at 4°C. Supernatants containing 400 to 500 $\mu$g proteins were incubated with a rabbit anti-TRPV3 antibody (1:100, raised by immunizing rabbits with a

protein encoding amino acids 326–340 of mouse TRPV3). TRPV4 proteins were detected by Western blot analysis using a rabbit anti-TRPV4 antibody (1:500, ab39260; Abcam).

**Western Blot.** For Western blot assay, after immunoprecipitation, protein samples were loaded and separated by SDS-PAGE and transferred onto polyvinylidene fluoride (PVDF) membranes (Millipore). After blocking with 5% nonfat milk in Tris-buffered saline-Tween for 1 hour at room temperature, membranes were incubated with rabbit anti-TRPV3 antibody (1:500, raised by immunizing rabbits with a protein encoding amino acids 326–340 of mouse TRPV3); mouse monoclonal anti-Flag (1:2000, F1804); rabbit anti-TRPV4 antibody (1:500, ab39260); or mouse monoclonal anti-actin (1:2000, sc-8432; Santa Cruz Biotechnology) at 4°C overnight. The membranes were incubated with their corresponding secondary horseradish peroxidase (HRP)-conjugated antibodies and detected using an enhanced chemiluminescence (ECL) Western blot detection system (Bio-Rad).

**Electrophysiology.** Whole-cell or single-channel patch clamp recordings were carried out using an EPC10 amplifier driven by the Patch Master software (HEKA, Bolanden, Germany) in the cell-free inside-out or whole-cell configuration. For both configurations, the bath solution and the pipette solution contained 130 mM NaCl, 3 mM HEPES, and 0.2 mM EDTA at pH 7.2. All recordings were performed at room temperature of 22 ± 2°C. TRPV3 agonist 2-aminoethoxydiphenyl borate (2-APB) and TRPV4 agonist GSK1016790A were applied to the patch using a rapid solution changer (RSC-200; Bio-Logic). The speed of solution exchange was estimated by monitoring the time course of junction potential change that occurred at the tip of an open pipette. Solution exchange was always completed within 100 milliseconds. All data are expressed as the mean ± S.D. An $EC_{50}$ was derived from fitting the dose-response relationship to a Hill equation. OriginPro 2019b (Origin Laboratory) was used for data analysis.

For the measurement of channel activation threshold by temperature, currents were recorded in whole-cell patch clamp configuration in response to a protocol consisting of a 300-millisecond step to +80 mV followed by a 300-millisecond step to −80 mV from holding potential (0 mV) at 1-second intervals. For temperature control, the bath solution was precooled to 20 ± 1°C and heated using a dual-channel temperature controller (Model TC-344C; Warner Instruments). The patch pipette was placed about 1 mm from the monitor thermistor (Model CC-28; Warner Instruments) to ensure accurate monitoring of local bath solution temperature. Temperature readout of the thermistor was fed into an analog input of an amplifier with simultaneous recordings of currents. The rate of temperature rise was set at a moderate rate of about 0.3°C/s for ensuring a steady recording of currents. With this method, we achieved a rapid and reliable temperature change between 20 and 45°C (Nie et al., 2021).

The precise heat activation threshold of temperature was analyzed using the method previously reported (Cheng et al., 2012). Briefly, we plotted the current against the reciprocal of the Kelvin temperature in a log scale. Linear curve fittings were operated between the range of leak currents and heat-activated channel currents. The demarcation of leak currents and heat-activated channel currents was the point at which the heat-activated TRPV3, TRPV4, and TRPV3/4 currents took off upon heating at about 32, 25, and 28°C, respectively. The exact value of temperature threshold for channel activation is obtained from the intersection of the pair of linear curves fitted to the leak currents and the heat-activated channel currents. The 95% confidence intervals for the interception of the linear curve fitting were as follows: 2.20 ± 0.09 for leak currents and 18.29 ± 0.20 for heat-activated TRPV3 currents; 0.07 ± 0.60 for leak currents and 20.90 ± 0.19 for heat-activated TRPV3/4 currents; and 1.06 ± 0.50 and 9.71 ± 0.16 for leak currents and heat-activated TRPV4 currents. Data are expressed as the means ± S.D., and the intersection values were derived from averages of individual curves. The $Q_{10}$ was used to characterize the temperature dependence of ionic current from calculation using the following equation:

$$Q_{10} = \left(\frac{I_2}{I_1}\right)^{10/(T_2 - T_1)} \quad (1)$$

where $I_2$ is the current at the higher temperature $T_2$ and $I_1$ is the current at the lower temperature $T_1$ (Gracheva et al., 2010). Data display was performed using Igor Pro 6.0 and OriginPro 2019b.

**Statistical Analysis.** All data are expressed as the means ± S.D. Statistical analyses were performed with Prism 8.0 software. Differences between experimental and control groups were compared using one-way ANOVA followed by Tukey multiple comparison test or two-way ANOVA followed by Bonferroni's multiple-comparison tests. Statistical significance was set at $P < 0.05$.

## Results

**Colocalization and Association of TRPV3 and TRPV4 Subunits.** To test if TRPV3 and TRPV4 subunits are colocalized, we started examining the expression of both TRPV3 and TRPV4 in HEK293 cells cotransfected with cDNAs encoding TRPV3-EYFP and mCherry-TRPV4 channels. Confocal imaging revealed that both TRPV3 and TRPV4 proteins were robustly expressed and colocalized in the cell surface and cytoplasm (Fig. 1A). Further immunoprecipitation with TRPV3 antibodies showed that Flag-TRPV4 proteins were detected from lysates of HEK293 cells coexpressing different ratios of TRPV3-EYFP and Flag-TRPV4 channels (Fig. 1B) compared with no TRPV4 protein bands detected in cells expressing either TRPV3-EYFP or Flag-TRPV4 alone after immunoprecipitation with anti-TRPV3 antibody (Fig. 1B). These results suggest that TRPV3 and TRPV4 subunits are colocalized in heterologously expressed cells and can biochemically interact.

To confirm if TRPV3 and TRPV4 can associate in native cells, we also performed coimmunoprecipitation of lysates from the mouse skin tissues after validating the specificity of TRPV3 antibody that is used to detect TRPV3 proteins in the mouse lysates of skin, liver, and heart tissues. TRPV3 is expressed in the skin with a protein band at about 100 kDa but not in liver and heart tissues that were used as negative controls (Supplemental Fig. 1). For coimmunoprecipitation, homogenates were prepared from wild-type (WT) TRPV3 or TRPV3 knockout (KO) mouse skin tissues for immunoprecipitation with anti-TRPV3 antibodies. TRPV4 proteins after immunoprecipitation with anti-TRPV3 antibodies were detected in the tissue homogenates from WT mice by anti-TRPV4 antibodies but were almost undetectable in TRPV3 KO mice (Fig. 1C). These results indicate that both TRPV3 and TRPV4 proteins can physically associate in both HEK293 cells and native skin tissues.

**The C Terminus Is Critical for the Interaction between TRPV3 and TRPV4 Channels.** To identify the domain critical for association between TRPV3 and TRPV4 subunit proteins, we used the membrane-tethered peptide Gap43 fused with either TRPV4 C terminus (Gap43-TRPV4 CT, residues 749–871) or TRPV4 N-terminal ankyrin repeat domain (Gap43-TRPV4 ARD, residues 149–396) as a bait to prey on either TRPV3 N-terminal ARD (TRPV3 ARD-EYFP, residues 118–367) or TRPV3 C terminus (TRPV3 CT-EYFP, residues 709–791) tagged with EYFP at their C terminus (Fig. 2A). The N-terminal ankyrin repeat domain (ARD) contains six ankyrin repeats, a common motif with typically 33 residues in each repeat (Shi et al., 2013; Singh et al., 2018). The Gap43 is 20 amino acids long, containing a signal for post-

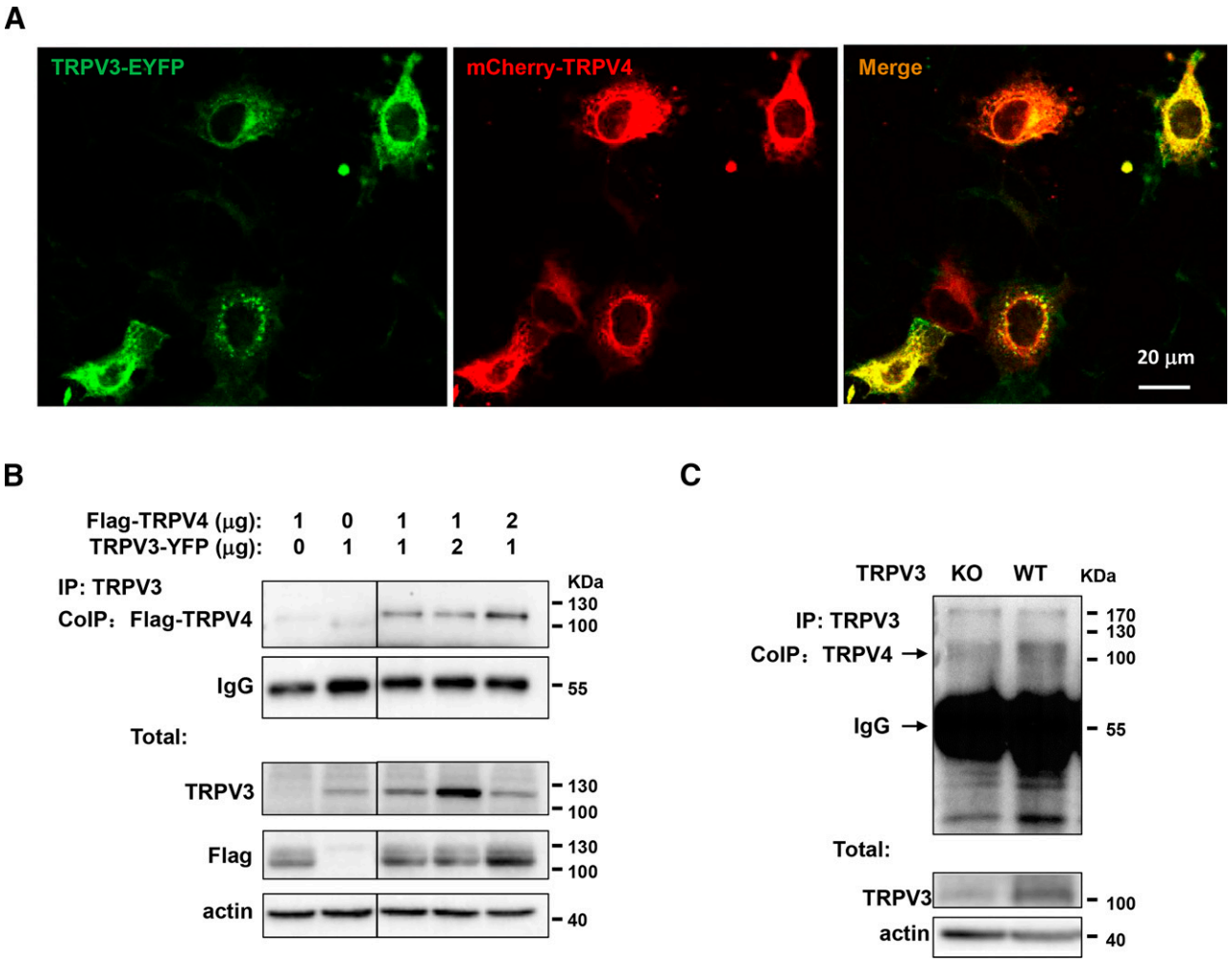


**Fig. 1.** Association between TRPV3 and TRPV4 proteins in HEK293 cells and mouse skin tissues. (A) Confocal imaging of TRPV3 (left panel in green), TRPV4 (middle panel in red), and their colocalization (right panel in orange) in HEK293 cells transiently transfected with TRPV3-EYFP and mCherry-TRPV4. TRPV3 and TRPV4 proteins are robustly expressed and colocalized in the cytoplasm and the cell surface. Scale bar, 20 μm. (B) Coimmunoprecipitation of lysates from HEK293T cells coexpressing Flag-TRPV4 and TRPV3-EYFP were immunoprecipitated with an anti-TRPV3 antibody. Lysates of cells expressing Flag-TRPV4 or TRPV3-EYFP were used as controls. Immunoblots were probed with an anti-Flag antibody. Total protein represents the direct immunoblotting of the lysates. (C) The presence of TRPV4 associated with TRPV3 in mouse skin. Lysates from skin of TRPV3-knockout or WT mice were immunoprecipitated with TRPV3 antibody before immunoblot with TRPV4 antibody.

translational palmitoylation of cysteines targeting and tethering to the membrane (Benowitz and Routtenberg, 1997; Zhang et al., 2011). We reasoned that if there was an interaction between the channel N-terminal ARD and/or C terminus, we would be able to detect the fluorescence at the membrane as a result of interaction between Gap43-CT/ARD and its associated proteins upon their coexpressions (Fig. 2A). When coexpressed with TRPV3 CT-EYFP, the membrane-tethered Gap43-TRPV4 CT but not the Gap43-tagged TRPV4 N-terminal ARD resulted in redistributing the TRPV3 CT-EYFP proteins on the membrane surface (Fig. 2B, top panels), indicating the interaction between TRPV3 C terminus and TRPV4 C terminus. However, coexpression of the membrane-tethered Gap43-TRPV4 ARD and TRPV3 CT-EYFP or TRPV3 ARD-EYFP gave rise to no redistribution of fluorescence compared with TRPV3 ARD-EYFP alone (Fig. 2B, bottom panels). These results demonstrate an interaction between TRPV3 and TRPV4 mediated by their C termini but not their N termini.

**Functional Assembly of TRPV3 and TRPV4 Channels Is Characterized by an Intermediate Single-Channel Conductance.** Homomeric TRPV3 and TRPV4 channels are characterized by different single-channel conductance at 175 picosiemens (pS) and 85 pS, respectively (Ma et al., 2011; Cheng et al., 2012). To determine the functional assembly between TRPV3 and TRPV4 channels, we performed single-channel recordings at +80 mV of inside-out patches excised from HEK293 cells expressing individual TRPV3 and TRPV4 or TRPV3 and TRPV4 channels together. The single-channel analysis revealed the single-channel conductance of homomeric TRPV3 channels at 176.1 ± 15.20 pS (Fig. 3A) and homomeric TRPV4 channels at 82.96 ± 4.45 pS (Fig. 3B). In contrast, the single-channel currents recorded from HEK293 cells coexpressing TRPV3 and TRPV4 channels exhibited distinct channel openings (Fig. 3C, O2) different from either TRPV3 channels (Fig. 3A, O1 and O2; Fig. 3C, O1) or TRPV4 channels (Fig. 3B, O1 and O2; Fig. 3C, O3). The distinct single-channel opening

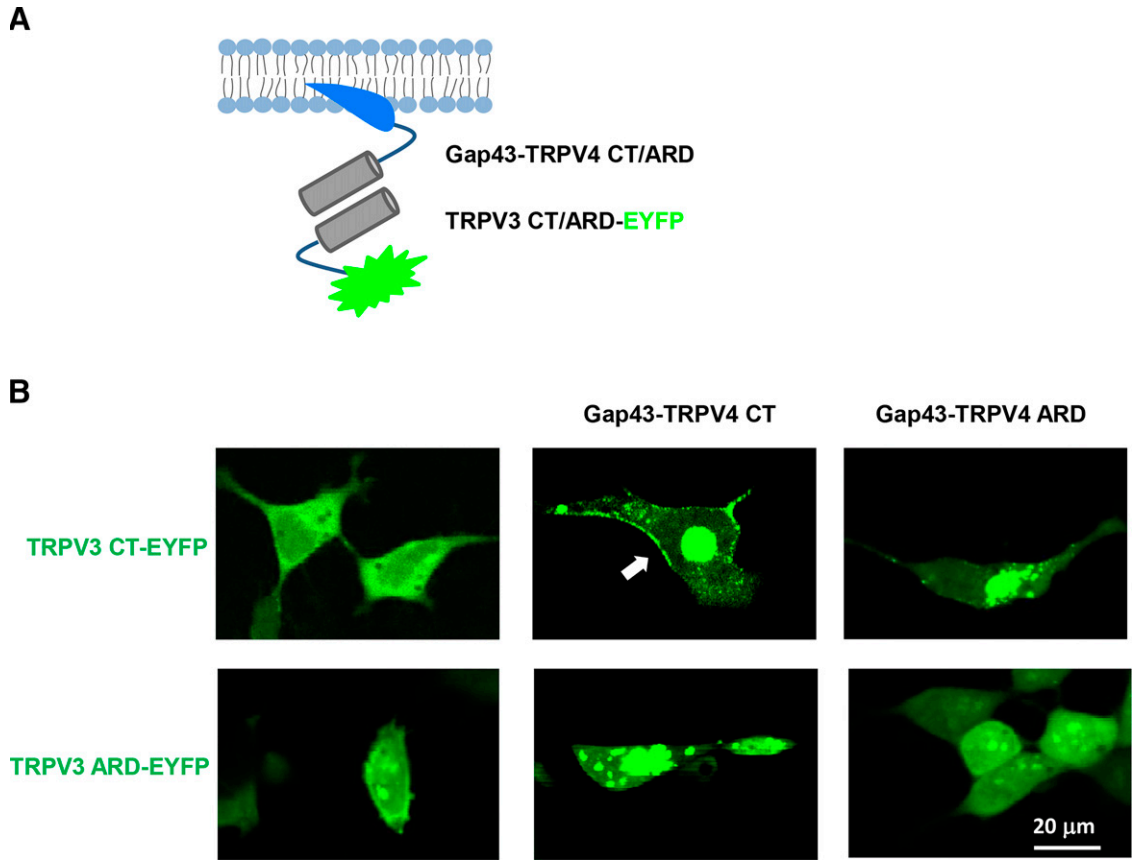


**Fig. 2.** The interaction mediated by TRPV3 and TRPV4 C termini in confocal imaging of HEK293 cells. (A) Schematic illustration for biochemical constructs testing the interaction between the Gap43 fused with TRPV4 C terminus or N-terminal ankyrin repeat domain (ARD) and TRPV3 C terminus or ARD tagged with EYFP. (B) Confocal images from HEK293 cells transfected with the constructs from (A). In the top panels, fluorescent imaging of HEK293 cells transfected with TRPV3 CT-EYFP alone as a control (left panel), cotransfected with TRPV3 CT-EYFP/Gap43-TRPV4 CT (middle panel), and TRPV3 CT-EYFP/Gap43-TRPV4 ARD (right panel). The membrane-tethered Gap43 fused with TRPV4 C terminus (a white arrow in middle panel) but not the Gap43-tagged TRPV4 N-terminal ARD (right panel) was capable of redistributing EYFP-tagged TRPV3 C terminus on the membrane surface. In the bottom panels, confocal imaging of fluorescence in HEK293 cells transfected with TRPV3 N-terminal ARD-EYFP alone as a control (left panel), cotransfected with TRPV3 ARD-EYFP/Gap43-TRPV4 CT (middle panel), and TRPV3 ARD-EYFP and Gap43-TRPV4 ARD (right panel). Coexpressing TRPV3 N-terminal ARD-EGFP with Gap43-tagged TRPV4 CT or TRPV4 ARD was unable to redistribute the surface expression. Scale bar, 20 $\mu$m.

yielded an intermediate single-channel conductance at 123.53 ± 3.19 pS (Fig. 3C), indicating a heterotetrameric assembly between TRPV3 and TRPV4 channels.

**Coassembled TRPV3 and TRPV4 Channel Complexes Are Characterized by Altered Pharmacology.** To confirm their functional coassembly of TRPV3 and TRPV4 channels, we used the tool agonist 2-aminoethoxydiphenyl borate (2-APB) that only activates WT TRPV3 channel but not WT TRPV4 channel. 2-APB can activate WT TRPV3 and TRPV4-N456H/W737R double mutant channels in concentration-dependent currents with $EC_{50}$ values of 58 $\mu$M [Hill slope ($n_{Hill}$) = 1.1] and 43 $\mu$M ($n_{Hill}$ = 1.3), respectively, but not a double mutant of TRPV3 (TRPV3-H426N/R696K) or WT TRPV4 channels (Table 1), consistent with the previous results (Hu et al., 2009). In contrast, coexpression of WT TRPV3 and TRPV3-H426N/R696K double mutant channels exhibited a reduced activation with an $EC_{50}$ of 192 $\mu$M ($n_{Hill}$ = 1.52) (Fig. 4A; Table 1). Similarly, coexpression of TRPV4-N456H/W737R and WT TRPV4 channels also gave rise to a reduced potency with $EC_{50}$ of 165 $\mu$M ($n_{Hill}$ = 1.77) (Fig. 4B; Table 1). Next, we recorded the whole-cell currents in HEK293 cells coexpressing TRPV3 and TRPV4 channels in the presence of 2-APB. As shown in Fig. 4C, adding different concentrations of 2-APB resulted in a concentration-dependent activation of coexpressed WT TRPV3 and WT TRPV4 channel currents with a distinct $EC_{50}$ of 212 $\mu$M ($n_{Hill}$ = 1.96) compared with the $EC_{50}$ of 58 $\mu$M ($n_{Hill}$ = 1.1) for WT TRPV3.

TRPV3 current exhibits a unique property of sensitization by repetitive applications of agonist 2-APB (Chung et al., 2004). To examine any alteration in the agonist-induced channel sensitization for coassembled TRPV3 and TRPV4 channel complexes, we repetitively applied 2-APB at 50 $\mu$M for 20 seconds with an interval of 40 seconds for each exposure. The results showed that coassembled TRPV3 and TRPV4 channel complexes showed a reduction of progressive current potentiation to repetitive 2-APB compared with an increased potentiation of homomeric TRPV3 channel currents (Fig. 4, D and E), although TRPV3/4 channels exhibited no obvious reduction of outward current rectification (Fig. 4F).

To further corroborate the functional coassembly of TRPV3 and TRPV4 channels, we tested the effects of a TRPV4-specific agonist GSK1016790A on activating TRPV3/4 channels Willette et al., 2008). Compared with the activation of homomeric TRPV4 channels, GSK1016790A at the same concentration of 100 nM led to a reduced activation of TRPV3/4 heterotetramers in both inward and outward

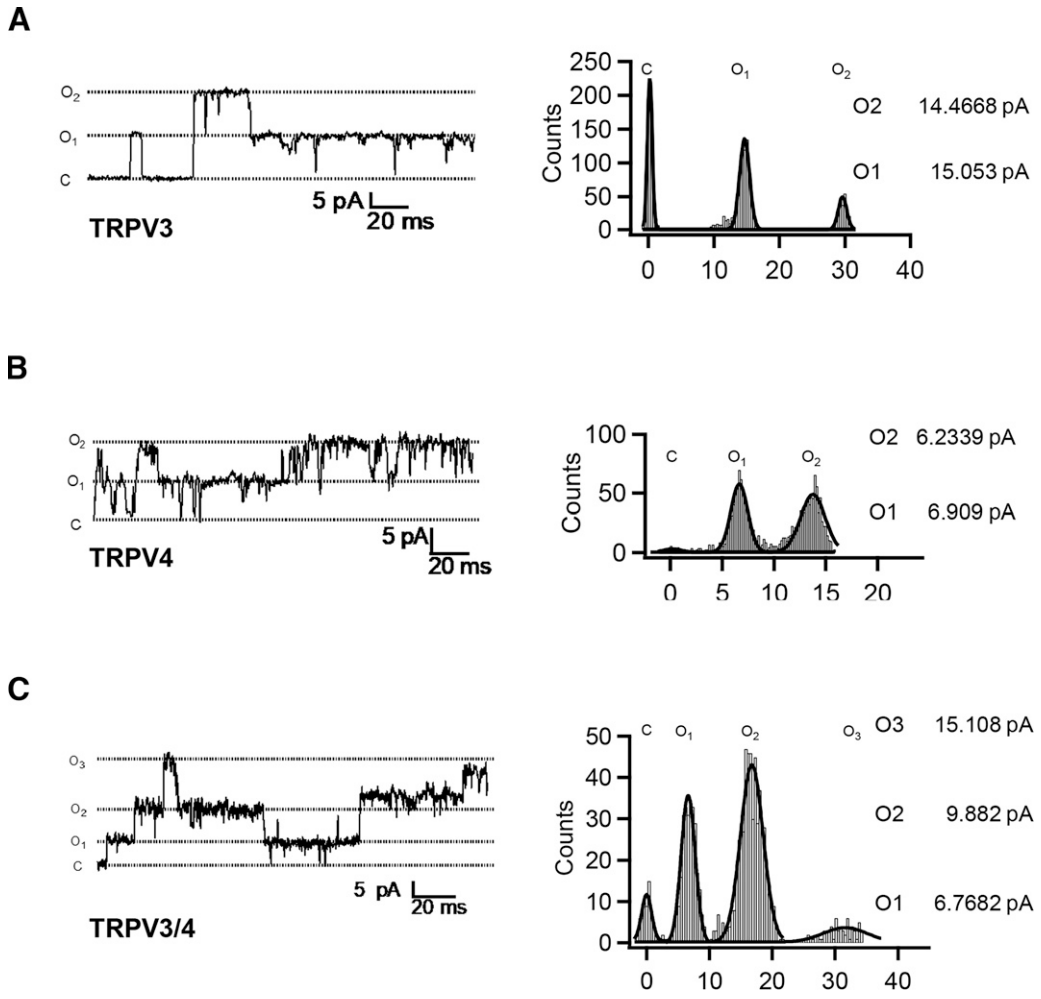


**Fig. 3.** A distinct intermediate single-channel conductance form ed by heterotetrameric assembly of TRPV3 and TRPV4 channels. (A–C, left panels) Representative recordings of single channels in cells held at +80 mV in inside-out patch configuration. Two or three channels were observed in each patch. Dashed lines represent different closing or opening states of single channels. The letter C represents closing state; O1, O2, and O3 represent different opening states. (A–C, right panels) Histogram of single-channel current amplitudes obtained under each condition as shown in their left panels; $n$ = 3–5.

currents (Fig. 4, G–I). All of these results demonstrated the functional assembly of heterotetrameric TRPV3 and TRPV4 channels to be pharmacologically different from their homotetramers.

**TRPV3 and TRPV4 Channel Complexes Exhibit Distinct Threshold of Temperature Activation.** TRPV3 is activated by temperature at 32–39°C, and TRPV4 is activated at 25°C. To examine if coassembled TRPV3/TRPV4 channel complexes are activated by distinct temperature, we recorded heteromeric TRPV3/TRPV4 channel currents in response to different temperature in whole-cell patch clamp configuration. The results showed that homomeric TRPV3 channels were activated at the activation threshold of 31.89 ± 0.41°C (Fig. 5, A and D) and that homomeric TRPV4 channels were activated by warm temperature with the threshold of 25.06 ± 0.38°C (Fig. 5, B and D), which is in line with previous observations (Güler et al., 2002; Peier et al., 2002b; Watanabe et al., 2002). When coexpressed with TRPV3 and TRPV4, there was a different activation threshold of heterotetrameric TRPV3/TRPV4 channels at 28.12 ± 0.37°C compared with homomeric TRPV3 or TRPV4 channels (Fig. 5, C and D) (Güler et al., 2002; Watanabe et al., 2002), demonstrating a distinct temperature activation of heterotetrameric TRPV3/4 channels compared with homomeric TRPV3 or TRPV4 channels.

TABLE 1
Summary for dose-dependent activation of homomeric and heterotetrameric channels by agonist 2-APB
A representative $EC_{50}$ was shown, determined by fitting the dose-response relationship to a Hill equation.

| Channel | $EC_{50}$ ($\mu$M) | $n_{Hill}$ |
|---|---|---|
| TRPV3 | 58 | 1.1 |
| TRPV3-H426N/R696K | No activation | Not applicable |
| TRPV3 and TRPV3-H426N/R696K | 192 | 1.52 |
| TRPV4 | No activation | Not applicable |
| TRPV4-N456H/W737R | 43 | 1.3 |
| TRPV4 and TRPV4-N456H/W737R | 165 | 1.77 |
| TRPV3 and TRPV4 | 212 | 1.96 |

## Discussion

The goal of this study was to test whether two thermo-TRPV channels, TRPV3 and TRPV4, can coassemble to form functional heterotetrameric channels. Our findings show that TRPV3 and TRPV4 channels can associate via their C termini to form functional channel complexes with an intermediate single-channel conductance, distinct temperature activation threshold, and altered pharmacology. The functional assembly of thermo-TRPV3 and TRPV4 channels may help explain the molecular basis for fine-tuning of temperature sensation and chemical perception in mammals.

Heteromeric TRP channels are ubiquitous with unique biophysical and pharmacological properties distinct from

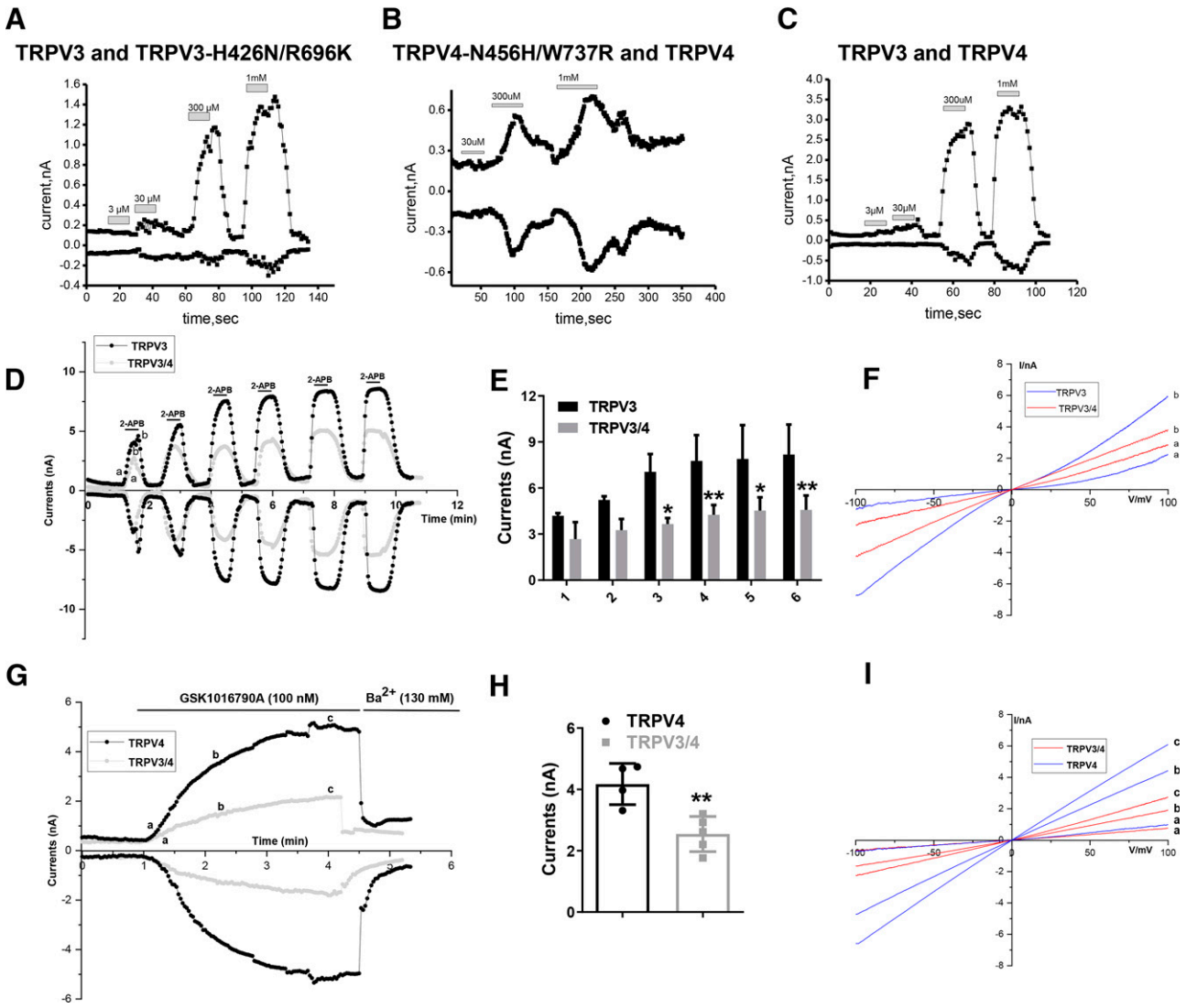


**Fig. 4.** (A–C) Altered pharmacological activation of functional TRPV3/4 channel complexes. Concentration-dependent activation of TRPV3/TRPV3-H426N/R696K channels (A), TRPV4-N456H/W737R/TRPV4 channels (B), or TRPV3/4 channels (C) coexpressed in HEK293 cells by 2-APB in whole-cell patch clamp recordings. Outward and inward currents were elicited at +80 and −80 mV, respectively, in the presence of different concentrations (3 $\mu$M–1 mM) of 2-APB. Their $EC_{50}$ values are for homomeric TRPV3 (58 $\mu$M, $n_{Hill}$ = 1.1); TRPV3/TRPV3-H426N/R696K (192 $\mu$M, $n_{Hill}$ = 1.52); TRPV4-N456H/W737R (43 $\mu$M, $n_{Hill}$ = 1.3); TRPV4-N456H/W737R/TRPV4 (165 $\mu$M, $n_{Hill}$ = 1.77); and heteromeric TRPV3/TRPV4 (212 $\mu$M, $n_{Hill}$ = 1.96) channels. Data are also shown in Table 1. (D) Representative current traces of TRPV3 and TRPV3/4 channels by repetitive applications of 2-APB at 50 $\mu$M for 20 seconds with an interval of 40 seconds in whole cell patch clamp recordings. Outward and inward currents were elicited at +80 and −80 mV, respectively. (E) Analysis of TRPV3 and TRPV3/4 peak currents evoked by six consecutive applications of 2-APB (50 $\mu$M). (F) I-V curves obtained from −100 to +100 mV voltage ramp at the times indicated in (D). (G) Representative current traces of TRPV4 and TRPV3/4 channels evoked by 100 nM GSK1016790A in whole-cell patch clamp recordings. Outward and inward currents were elicited at +80 and −80 mV, respectively. (H) Analysis for comparison of TRPV3 and TRPV3/4 peak currents evoked by GSK1016790A (100 nM). (I) I-V curves obtained from −100 to +100 mV voltage ramp at the times indicated in (G). Data are expressed as the means ± S.D. ($n$ = 3–5) and analyzed by two-way ANOVA followed by the Bonferroni's multiple-comparisons tests (E) or unpaired $t$ test (H); *$P < 0.05$, **$P < 0.01$.

homomeric channels. Coassembly of TRP and TRPL in *Drosophila melanogaster* leads to a store-operated, outwardly rectifying current distinct from the TRP or TRPL channel (Xu et al., 1997). Coexpression of TRPC1 and TRPC3 results in the formation of oligomeric TRP channels with distinguishable $Ca^{2+}$ sensitivity (Lintschinger et al., 2000). TRP$\gamma$ preferentially heteromultimerizes with TRPL in vitro and in vivo, and the heteromultimers contribute to the photoresponse (Xu et al., 2000). TRPC1 and TRPC5 are heteromeric subunits of a neuronal channel in the hippocampus, and in vitro coexpression of TRPC1 and TRPC5 results in a novel nonselective cation channel with voltage dependence similar to N-methyl-D-aspartate (NMDA) receptor channels but unlike that of any reported TRPC channel (Strübing et al., 2001). TRPP2 and TRPC1 assemble to form a channel with a unique constellation of new and TRPP2/TRPC1-specific properties (Bai et al., 2008). TRPM6 and TRPM7 are two known channel kinases. TRPM6 forms functional heteromeric channels in combination with TRPM7 with several unique functional characteristics (Li et al., 2006). TRP mucolipin 3 (TRPML3) and TRPV5 form heteromeric channels with a different conductance (Guo et al., 2013). Heteromeric assembly has also been demonstrated between TRPV subfamily members, such as heteromeric TRPV1/3 channels exhibiting an intermediate conductance, lower sensitivity to capsaicin,

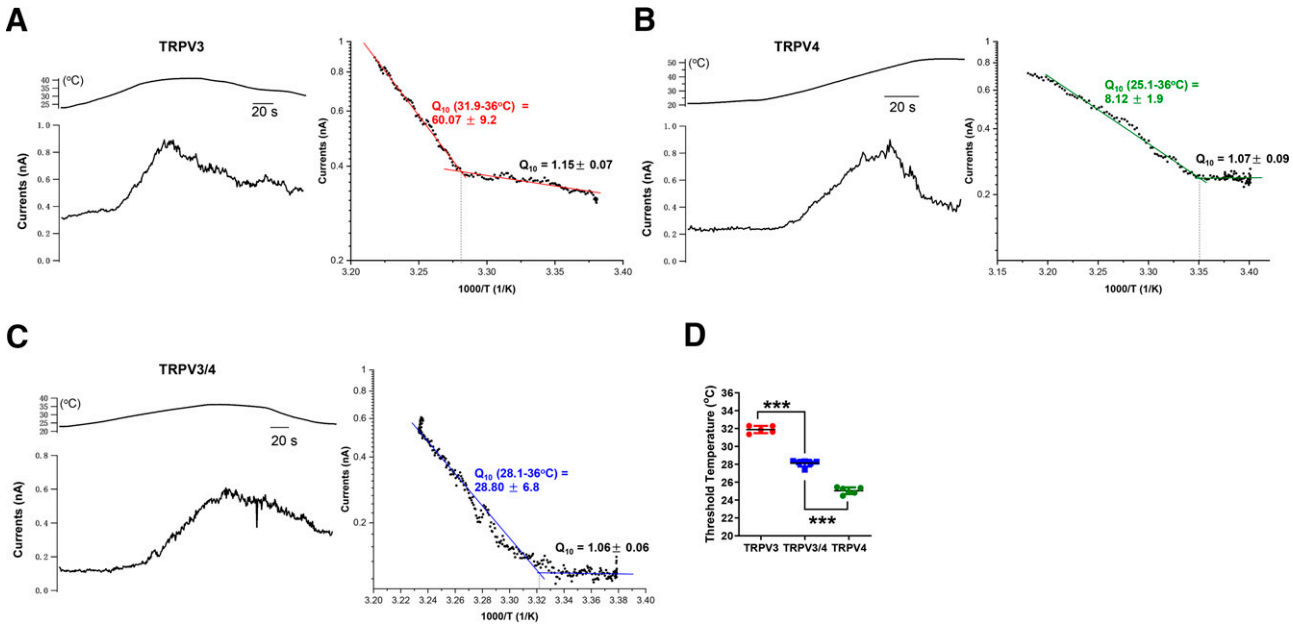


**Fig. 5.** (A–C, left panels) TRPV3, TRPV4, and TRPV3/TRPV4 channels exhibit distinct heat-activation thresholds. Representative current traces of temperature-dependent activation of TRPV3 (A), TRPV4 (B), and TRPV3/4 (C) channels recorded at +80 mV; right panels, plots showing their temperature thresholds and $Q_{10}$ values for leak currents and heat-activated channel currents. The temperature threshold for channel activation is defined as the intersection of the pair of linear curves fitting to the leak currents and the heat-activated channel currents. (D) Summary for analysis of temperature-activation threshold of homomeric TRPV3 (31.89 ± 0.41°C, $n = 5$); heteromeric TRPV3/TRPV4 (28.12 ± 0.37°C, $n = 6$); and homomeric TRPV4 channels (25.05 ± 0.38°C, $n = 6$). Data are expressed as the means ± S.D. and analyzed by ANOVA followed by the Tukey multiple comparison test; ***$P < 0.001$.

and distinct temperature activation threshold (Cheng et al., 2007, 2012).

In this study we used the membrane-tethered Gap43 peptide fused with channel domains for identification of TRPV3 and TRPV4 subunit interactions (Zhang et al., 2011; Lei et al., 2013). We find that the membrane-tethered Gap43-TRPV4 CT is capable of redistributing the TRPV3 CT-EGFP proteins on the membrane, indicating that the heteromeric assembly between TRPV3 and TRPV4 subunits is mediated by their C termini, consistent with the observation that a conserved tetramerization assembly domain in C terminus of TRPV1–4 mediates the assembly of homomeric channels (Zhang et al., 2011) before further modification and maturation in Golgi (Lei et al., 2013). Our coimmunoprecipitation (co-IP) experiments show that TRPV3 and TRPV4 proteins can physically associate in native skin tissues. However, in TRPV3 KO skin tissue samples, there was a faint band in predicted size that may result from the pulldown of other proteins in the skin tissues. Functional evaluation reveals a proximate intermediate single-channel conductance of about 123 pS that is unique compared with either 176.1 pS of unitary conductance for homomeric TRPV3 or 82.96 pS for homomeric TRPV4. As a single-channel conductance is a signature for a functional ion channel, the altered single conductance indicates the functional coassembly of TRPV3 and TRPV4 channels, which is also consistent with the intermediate single-channel conductance resulted from coassembly between Slack and Slo channels (Joiner et al., 1998) or *Shaker* WT channels and their T442S mutants (Zheng and Sigworth, 1998). Intermediate single-channel conductance is also observed in heterotetrameric TWIK-related $K^+$ (TREK)-2-S/TREK-1-L channels, TRP mucolipin 3 (TRPML3)/TRPV5 channels, TRPM6/7 channels, and TRPV1/3 channels (Li et al., 2006; Cheng et al., 2012; Guo et al., 2013; Lengyel et al., 2016).

Theoretically, TRPV3 and TRPV4 coexpressed in cells may randomly form homotetrameric or heterotetrameric channels with different subunit stoichiometry (three TRPV3 and one TRPV4, two TRPV3 and two TRPV4, one TRPV3 and three TRPV4). In this study, we coexpressed TRPV3 and TRPV4 at 1:1 ratio and observed the single-channel conductance at approximately 123.53 pS. This intermediate conductance might represent the heterotetrameric channel complexes composed of two TRPV3 and two TRPV4 subunits. It is also possible that other intermediate single-channel conductance can be formed through combinations of three TRPV3 and one TRPV4 or one TRPV3 and three TRPV4 subunits.

The channel pharmacology is another critical characteristic for heteromeric subunit assembly. Heterodimers formed by TREK-1 and TREK-2 are characterized by intermediate ruthenium red sensitivity (Lengyel et al., 2016). Tandem TREK1/TRAAK (TWIK-related arachidonic acid–stimulated $K^+$) channels display an intermediate activation profile of ML67 (a potent activator of TREK1 and TRAAK channels) and a lesser sensitivity than TREK1 of fluoxetine (an inhibitor of TREK1 with no effect on TRAAK current) (Blin et al., 2016). Micromolar levels of 2-APB maximally enhance TRPM6 and slightly increase TRPM6/7 but significantly inhibit TRPM7 channel activities, whereas millimolar concentrations of 2-APB increase TRPM6/7 and TRPM7 channel activities (Li et al., 2006). Coassembly of TRPV1 and TRPV3 subunits yields heteromeric channels with lesser sensitivity of TRPV1-specific agonist capsaicin compared with TRPV1 channel (Cheng et al., 2007, 2012). TRPV1-specific antagonist capsazepine causes a significant shift of the half-activation voltage of TRPV1/3 heterotetramer to a more depolarized direction than

TRPV1 (Cheng et al., 2012). Our findings show that coassembly of heterotetrameric TRPV3/TRPV4 channels features less sensitivity to agonist 2-APB. The reduced sensitization of TRPV3/4 heterotetramers to 2-APB likely results from a reduction of two 2-APB binding sites in TRPV3/4 heterotetramers compared to four 2-APB binding sites in homomeric TRPV3 (Cheng et al., 2012). The heterotetrameric TRPV3/TRPV4 channels show less sensitization than that of TRPV3 during repetitive applications of 2-APB. In addition, we show that active heterotetrameric TRPV3/TRPV4 channels are less sensitive to TRPV4-specific agonist GSK1016790A, which can robustly activate the homomeric TRPV4 channel. The altered pharmacology further indicates that TRPV3 and TRPV4 can coassemble into functional channel complexes.

Each thermo-TRP is activated at a specific temperature range. However, how they work together to detect a wide temperature change from noxious heat (>52°C) to noxious cold (<10°C) is still unknown (Dhaka et al., 2006; Kashio, 2021). Here we show a distinct activation threshold of TRPV3/4 heterotetrameric channels, which is distinguishable from homomeric TRPV3 or TRPV4 channels. The outer pore region has been suggested to be involved in temperature-dependent gating and thermal activation process of thermo-TRPs (Grandl et al., 2008; Yang et al., 2010; Du et al., 2020). The different temperature activation of heterotetrameric TRPV3/4 channels may result from the formation of distinct pore structure. The heterotetrameric TRPV3/4 channels with different threshold of temperature activation likely serve to increase functional channel diversity within the subfamily, which may underlie the mechanisms for fine-tuning of temperature sensation.

In conclusion, we demonstrated that two innocuous warmth-sensitive thermoreceptors, TRPV3 and TRPV4, can assembly into heterotetrameric functional channels characterized by an intermediate single-channel conductance, distinct temperature activation threshold, and altered channel pharmacology. Our findings reveal a role of heteromeric assembly of TRP channels in physiologic fine-tuning of temperature or chemical detection and sensation. In addition, pharmacological inhibition of either TRPV3 or TRPV4 may serve as a therapeutic strategy for suppressing the functional channel complexes in channelopathies.

#### Acknowledgments

The authors are very grateful for the assistance in whole-cell recordings from Mr. H. Zhang in Dr. F. Yang's laboratory at Zhejiang University. The authors also thank H. Wu, Y.Y. Nie, N.N. Wei, X.Y. Sun, and Y.H. Tian of laboratory members for technical assistance.

#### Authorship Contributions

*Participated in research design:* Hu, Wang.
*Conducted experiments:* Hu, Cao, Niu.
*Performed data analysis:* Hu, Cao.
*Wrote or contributed to the writing of the manuscript:* Hu, Wang.

#### References

Bai CX, Giamarchi A, Rodat-Despoix L, Padilla F, Downs T, Tsiokas L, and Delmas P (2008) Formation of a new receptor-operated channel by heteromeric assembly of TRPP2 and TRPC1 subunits. *EMBO Rep* **9**:472–479.
Bandell M, Macpherson LJ, and Patapoutian A (2007) From chills to chilis: mechanisms for thermosensation and chemesthesis via thermoTRPs. *Curr Opin Neurobiol* **17**:490–497.
Benowitz LI and Routtenberg A (1997) GAP-43: an intrinsic determinant of neuronal development and plasticity. *Trends Neurosci* **20**:84–91.
Blin S, Ben Soussia I, Kim EJ, Brau F, Kang D, Lesage F, and Bichet D (2016) Mixing and matching TREK/TRAAK subunits generate heterodimeric K2P channels with unique properties. *Proc Natl Acad Sci USA* **113**:4200–4205.
Caterina MJ, Rosen TA, Tominaga M, Brake AJ, and Julius D (1999) A capsaicin-receptor homologue with a high threshold for noxious heat. *Nature* **398**:436–441.
Caterina MJ, Schumacher MA, Tominaga M, Rosen TA, Levine JD, and Julius D (1997) The capsaicin receptor: a heat-activated ion channel in the pain pathway. *Nature* **389**:816–824.
Cheng W, Yang F, Liu S, Colton CK, Wang C, Cui Y, Cao X, Zhu MX, Sun C, Wang K, et al. (2012) Heteromeric heat-sensitive transient receptor potential channels exhibit distinct temperature and chemical response. *J Biol Chem* **287**:7279–7288.
Cheng W, Yang F, Takanishi CL, and Zheng J (2007) Thermosensitive TRPV channel subunits coassemble into heteromeric channels with intermediate conductance and gating properties. *J Gen Physiol* **129**:191–207.
Cheng X, Jin J, Hu L, Shen D, Dong XP, Samie MA, Knoff J, Eisinger B, Liu ML, Huang SM, et al. (2010) TRP channel regulates EGFR signaling in hair morphogenesis and skin barrier formation. *Cell* **141**:331–343.
Chung MK, Lee H, Mizuno A, Suzuki M, and Caterina MJ (2004) 2-aminoethoxydiphenyl borate activates and sensitizes the heat-gated ion channel TRPV3. *J Neurosci* **24**:5177–5182.
Dhaka A, Viswanath V, and Patapoutian A (2006) Trp ion channels and temperature sensation. *Annu Rev Neurosci* **29**:135–161.
Du G, Tian Y, Yao Z, Vu S, Zheng J, Chai L, Wang K, and Yang S (2020) A specialized pore turret in the mammalian cation channel TRPV1 is responsible for distinct and species-specific heat activation thresholds. *J Biol Chem* **295**:9641–9649.
Gracheva EO, Ingolia NT, Kelly YM, Cordero-Morales JF, Hollopeter G, Chesler AT, Sánchez EE, Perez JC, Weissman JS, and Julius D (2010) Molecular basis of infrared detection by snakes. *Nature* **464**:1006–1011.
Grandl J, Hu H, Bandell M, Bursulaya B, Schmidt M, Petrus M, and Patapoutian A (2008) Pore region of TRPV3 ion channel is specifically required for heat activation. *Nat Neurosci* **11**:1007–1013.
Güler AD, Lee H, Iida T, Shimizu I, Tominaga M, and Caterina M (2002) Heat-evoked activation of the ion channel, TRPV4. *J Neurosci* **22**:6408–6414.
Guo Z, Grimm C, Becker L, Ricci AJ, and Heller S (2013) A novel ion channel formed by interaction of TRPML3 with TRPV5. *PLoS One* **8**:e58174.
Hu H, Grandl J, Bandell M, Petrus M, and Patapoutian A (2009) Two amino acid residues determine 2-APB sensitivity of the ion channels TRPV3 and TRPV4. *Proc Natl Acad Sci USA* **106**:1626–1631.
Joiner WJ, Tang MD, Wang LY, Dworetzky SI, Boissard CG, Gan L, Gribkoff VK, and Kaczmarek LK (1998) Formation of intermediate-conductance calcium-activated potassium channels by interaction of Slack and Slo subunits. *Nat Neurosci* **1**:462–469.
Kashio M (2021) Thermosensation involving thermo-TRPs. *Mol Cell Endocrinol* **520**:111089.
Lapajne L, Lakk M, Yarishkin O, Gubeljak L, Hawlina M, and Križaj D (2020) Polymodal sensory transduction in mouse corneal epithelial cells. *Invest Ophthalmol Vis Sci* **61**:2.
Laursen WJ, Anderson EO, Hoffstaetter LJ, Bagriantsev SN, and Gracheva EO (2015) Species-specific temperature sensitivity of TRPA1. *Temperature* **2**:214–226.
Lei L, Cao X, Yang F, Shi DJ, Tang YQ, Zheng J, and Wang K (2013) A TRPV4 channel C-terminal folding recognition domain critical for trafficking and function. *J Biol Chem* **288**:10427–10439.
Lengyel M, Czirják G, and Enyedi P (2016) Formation of functional heterodimers by TREK-1 and TREK-2 two-pore domain potassium channel subunits. *J Biol Chem* **291**:13649–13661.
Li M, Jiang J, and Yue L (2006) Functional characterization of homo- and heteromeric channel kinases TRPM6 and TRPM7. *J Gen Physiol* **127**:525–537.
Lin Z, Chen Q, Lee M, Cao X, Zhang J, Ma D, Chen L, Hu X, Wang H, Wang X, et al. (2012) Exome sequencing reveals mutations in TRPV3 as a cause of Olmsted syndrome. *Am J Hum Genet* **90**:558–564.
Lintschinger B, Balzer-Geldsetzer M, Baskaran T, Graier WF, Romanin C, Zhu MX, and Groschner K (2000) Coassembly of Trp1 and Trp3 proteins generates diacylglycerol- and Ca2+-sensitive cation channels. *J Biol Chem* **275**:27799–27805.
Liu Y, Yan X, Chen Y, He Z, and Ouyang Y (2020) Novel TRPV4 mutation in a large Chinese family with congenital distal spinal muscular atrophy, skeletal dysplasia and scaly skin. *J Neurol Sci* **419**:117153.
Ma X, Nilius B, Wong JW, Huang Y, and Yao X (2011) Electrophysiological properties of heteromeric TRPV4-C1 channels. *Biochim Biophys Acta* **1808**:2789–2797.
Moqrich A, Hwang SW, Earley TJ, Petrus MJ, Murray AN, Spencer KS, Andahazy M, Story GM, and Patapoutian A (2005) Impaired thermosensation in mice lacking TRPV3, a heat and camphor sensor in the skin. *Science* **307**:1468–1472.
Nie Y, Li Y, Liu L, Ren S, Tian Y, and Yang F (2021) Molecular mechanism underlying modulation of TRPV1 heat activation by polyols. *J Biol Chem* **297**:100806.
Nilius B and Owsianik G (2011) The transient receptor potential family of ion channels. *Genome Biol* **12**:218.
Peier AM, Moqrich A, Hergarden AC, Reeve AJ, Andersson DA, Story GM, Earley TJ, Dragoni I, McIntyre P, Bevan S, et al. (2002a) A TRP channel that senses cold stimuli and menthol. *Cell* **108**:705–715.
Peier AM, Reeve AJ, Andersson DA, Moqrich A, Earley TJ, Hergarden AC, Story GM, Colley S, Hogenesch JB, McIntyre P, et al. (2002b) A heat-sensitive TRP channel expressed in keratinocytes. *Science* **296**:2046–2049.
Shi DJ, Ye S, Cao X, Zhang R, and Wang K (2013) Crystal structure of the N-terminal ankyrin repeat domain of TRPV3 reveals unique conformation of finger 3 loop critical for channel function. *Protein Cell* **4**:942–950.
Singh AK, McGoldrick LL, and Sobolevsky AI (2018) Structure and gating mechanism of the transient receptor potential channel TRPV3. *Nat Struct Mol Biol* **25**:805–813.
Smith GD, Gunthorpe MJ, Kelsell RE, Hayes PD, Reilly P, Facer P, Wright JE, Jerman JC, Walhin JP, Ooi L, et al. (2002) TRPV3 is a temperature-sensitive vanilloid receptor-like protein. *Nature* **418**:186–190.

Strübing C, Krapivinsky G, Krapivinsky L, and Clapham DE (2001) TRPC1 and TRPC5 form a novel cation channel in mammalian brain. *Neuron* **29**:645–655.

Szöllősi AG, Vasas N, Angyal Á, Kistamás K, Nánási PP, Mihály J, Béke G, Herczeg-Lisztes E, Szegedi A, Kawada N, et al. (2018) Activation of TRPV3 regulates inflammatory actions of human epidermal keratinocytes. *J Invest Dermatol* **138**:365–374.

Talavera K, Yasumatsu K, Voets T, Droogmans G, Shigemura N, Ninomiya Y, Margolskee RF, and Nilius B (2005) Heat activation of TRPM5 underlies thermal sensitivity of sweet taste. *Nature* **438**:1022–1025.

Tan CH and McNaughton PA (2016) The TRPM2 ion channel is required for sensitivity to warmth. *Nature* **536**:460–463.

Vay L, Gu C, and McNaughton PA (2012) The thermo-TRP ion channel family: properties and therapeutic implications. *Br J Pharmacol* **165**:787–801.

Vriens J, Nilius B, and Voets T (2014) Peripheral thermosensation in mammals. *Nat Rev Neurosci* **15**:573–589.

Vriens J, Owsianik G, Hofmann T, Philipp SE, Stab J, Chen X, Benoit M, Xue F, Janssens A, Kerselaers S, et al. (2011) TRPM3 is a nociceptor channel involved in the detection of noxious heat. *Neuron* **70**:482–494.

Watanabe H, Vriens J, Suh SH, Benham CD, Droogmans G, and Nilius B (2002) Heat-evoked activation of TRPV4 channels in a HEK293 cell expression system and in native mouse aorta endothelial cells. *J Biol Chem* **277**:47044–47051.

Willette RN, Bao W, Nerurkar S, Yue TL, Doe CP, Stankus G, Turner GH, Ju H, Thomas H, Fishman CE, et al. (2008) Systemic activation of the transient receptor potential vanilloid subtype 4 channel causes endothelial failure and circulatory collapse: part 2. *J Pharmacol Exp Ther* **326**:443–452.

Xu H, Ramsey IS, Kotecha SA, Moran MM, Chong JA, Lawson D, Ge P, Lilly J, Silos-Santiago I, Xie Y, et al. (2002) TRPV3 is a calcium-permeable temperature-sensitive cation channel. *Nature* **418**:181–186.

Xu XZ, Chien F, Butler A, Salkoff L, and Montell C (2000) TRPgamma, a drosophila TRP-related subunit, forms a regulated cation channel with TRPL. *Neuron* **26**:647–657.

Xu XZ, Li HS, Guggino WB, and Montell C (1997) Coassembly of TRP and TRPL produces a distinct store-operated conductance. *Cell* **89**:1155–1164.

Yang F, Cui Y, Wang K, and Zheng J (2010) Thermosensitive TRP channel pore turret is part of the temperature activation pathway. *Proc Natl Acad Sci USA* **107**:7083–7088.

Zhang F, Liu S, Yang F, Zheng J, and Wang K (2011) Identification of a tetrameric assembly domain in the C terminus of heat-activated TRPV1 channels. *J Biol Chem* **286**:15308–15316.

Zheng J and Sigworth FJ (1998) Intermediate conductances during deactivation of heteromultimeric Shaker potassium channels. *J Gen Physiol* **112**:457–474.

**Address correspondence to:** KeWei Wang, Qingdao University, 39 Dengzhou Road, Qingdao 266021, China. E-mail: wangkw@qdu.edu.cn

# Co-assembly of warm-temperature sensitive TRPV3 and TRPV4 channel complexes with distinct functional properties

Fang Hu, Xu Cao, Canyang Niu and KeWei Wang

## Supplemental Information

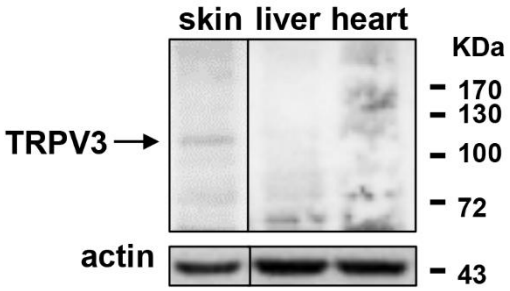


**Figure S1. Detection of TRPV3 protein expression in the mouse skin, liver and heart tissues by anti-TRPV3 antibody in western blot assay.** TRPV3 is expressed in the skin with a protein band at about 100 KDa, but not in the liver and heart tissues that were used as negative controls.